Research Square

Preprints are preliminary reports that have not undergone peer review.
They should not be considered conclusive, used to inform clinical practice,
or referenced by the media as validated information.

Hybrid WDM-PON/FSO/VLC Access Under Arid Conditions

Adnan Ali Abdullah

adnan.ali23@tu.edu.iq

University of Tikrit

Ahmed Saad Names

University of Tikrit

Research Article

Keywords: hybrid optical access network, WDM-PON, free-space optics, visible light communication, atmospheric turbulence, dust attenuation, last-mile connectivity

Posted Date: November 25th, 2026

DOI: https://doi.org/10.21203/rs.3.rs-10335986/v1

License: This work is licensed under a Creative Commons Attribution 4.0 International License.
Read Full License

Additional Declarations: No competing interests reported.

Hybrid WDM-PON/FSO/VLC Access Under Arid Conditions

Adnan Ali Abdullah[1]*, Ahmed Saad Names[1]

[1]Shirqat College of Engineering, Department of Electrical Engineering, University of Tikrit, Shirqat, Iraq

adnan.ali23@tu.edu.iq , ahmed.alnames@tu.edu.iq

Abstract

Hybrid optical access networks combining fiber, free-space optical (FSO), and visible light communication (VLC) promise high-capacity last-mile connectivity in arid regions, yet their behavior under dust and haze remains poorly understood. We address this with an end-to-end OptiSystem simulation of a three-tier WDM-PON/FSO/VLC architecture. The chain runs from a 20 km single-mode fiber backbone carrying four WDM channels at 100 GHz spacing (1547.6–1550 nm), through a 1 km outdoor FSO segment under the Gamma–Gamma turbulence model, to a 3 m indoor link fed by a 550 nm source. Performance is read through bit error rate (BER), quality (Q) factor, eye diagrams, and received optical power across five atmospheric conditions and sweeps in FSO distance, bit rate, fiber length, and VLC range. In clear weather the link is error-free, with BER under 10^{-9}. Light haze costs little: at 4.2 dB/km every channel stays beneath the forward-error-correction threshold. Dust is the breaking point—at ≥10 dB/km the 1 km link fails, and a heavy 127 dB/km storm shrinks usable FSO range below 200 m. By the VLC receiver the budget has fallen to −12.53 dBm. These results map where a dust-prone link can operate and pin the performance ceiling on one tier: FSO.

Keywords — *hybrid optical access network; WDM-PON; free-space optics; visible light communication; atmospheric turbulence; dust attenuation; last-mile connectivity.*

1. Introduction

Broadband demand keeps climbing steeply. 5G and beyond-5G rollouts, a proliferating Internet of Things (IoT), and the now-routine use of high-definition media have together pushed the optical access layer to sustain traffic volumes scarcely imaginable a decade ago [1], [2]. For the last mile, the passive optical network (PON) layered on wavelength-division multiplexing (WDM) leads the field. Its appeal is straightforward: it scales cleanly at low power, and a single shared feeder serves many subscribers at once [3]. Taking fiber all the way to every doorstep stays awkward, however, wherever settlement is thin, the ground is hostile, or digging is hemmed in by regulation [4].

One way past these barriers is to keep fiber where it is cheap to install and switch to wireless optical links everywhere else. Free-space optics (FSO) carries data at near-fiber rates while sparing the expense of laying cable, and visible light communication (VLC), or Li-Fi, repurposes the light-emitting diodes (LEDs) that already light a room to deliver dense, short-range coverage [5], [6]. Joining the three—WDM-PON for the backbone, FSO for the open-air hop, and VLC for the final indoor stretch—yields a natural blueprint for next-generation last-mile access [7]–[9].

Attractive as the three-tier idea is, its behavior in harsh climates has been examined far less often than the concept itself. FSO performance under fog, rain, and snow is by now well documented [10]–[12], but dust storms and suspended particulates—the conditions that define arid regions—have drawn comparatively little attention in the simulation literature. Field measurements in [13]–[15] show that attenuation during dust storms can climb to several hundred dB/km at near-infrared wavelengths, a regime in which FSO availability is severely tested. What has not been studied in any depth is how these dust effects play out when the FSO link sits between active WDM-PON and VLC tiers and the chain is evaluated from end to end.

To close that gap, this work simulates a full WDM-PON/FSO/VLC three-tier access network built for arid-climate operation. The starting point is a complete end-to-end OptiSystem model that chains a 20 km SMF backbone—four WDM channels at 100 GHz spacing—to a 1 km FSO segment under Gamma–Gamma turbulence and, finally, a 3 m indoor VLC link. We then run that model through five representative atmospheric scenarios, each with attenuation calibrated against published arid-environment measurements, and follow it with parametric sweeps over FSO distance, bit rate, fiber length, and indoor VLC range to expose which factor dominates in each tier. Two further pieces round out the study. A full link budget, derived and then checked against the simulated received powers, gives a concrete design reference for dust-prone sites; and the maximum usable FSO distance, quantified for every atmospheric condition, turns the analysis directly into deployment guidelines for last-mile optical access in arid regions.

From here, the System Model and Simulation Setup sections lay out the architecture, governing equations, parameters, and scenarios; the Results and Discussion section reports the performance evaluation; and the Link Budget Analysis and Conclusion sections account for the end-to-end power flow and gather the findings together with directions for future work.

2. Related Work

Hybrid access designs that fuse fiber, FSO, and VLC have drawn a steady stream of recent work. Lamba et al. [2] folded a wireless hop into a WDM-PON and, by multiplexing across polarization states and seeding the channels from a frequency comb, pushed the aggregate rate to 96 Gbps. Kumari [3] joined an NGPON backbone to an FSO span, lifted capacity through mode-division multiplexing, and traced how the wired and wireless losses add up. Aiming at cellular fronthaul, AlQahtani and El-Nahal [6], [7] built coherent links that marry WDM-PON with FSO; in one of their designs, LDPC decoding was enough to hold a 2 km hop steady through strong turbulence. Resilience has been tackled as well: Wu et al. [8] let a WDM access network heal itself by duplicating the fiber and FSO routes, so traffic keeps flowing when a fiber is severed, whereas Kumari et al. [9] laid the nodes of an 8 × 200 Gbps hybrid PON out in a wheel topology and folded the fiber and FSO impairments into each spoke.

Work on VLC and indoor optical wireless has advanced in parallel. Singh and Pandey [4] asked whether VLC could carry the low-latency traffic an indoor metaverse would demand, and Elamrawy et al. [16] measured how an indoor VLC link responds as the LED arrangement and the photodetector choice are varied. El-Garhy et al. [1] set a standalone VLC link against a combined FSO/VLC one and found that running the two together extends the dependable coverage distance without letting the error rate drift out of range. The FSO channel itself has

been charted in comparable depth under atmospheric stress: Kumari and Arya [10] examined an XG-PON link coupled to FSO, using Gamma–Gamma statistics to represent the channel in severe weather, while both Belgaonkar et al. [17] and Xu et al. [18] put numbers to FSO error rate and channel capacity under turbulence as the noise contributions were varied.

A smaller but growing line of work speaks directly to arid-climate deployment. Esmail et al. [15] pushed a 28 GHz 5G signal across a link that combines optical FSO with RF and showed it could ride out dusty conditions; Ali et al. [14] asked how much throughput an FSO link still delivers once dust sets in; and reference [11] introduces a general analytical model for FSO links whose fading is driven by airborne dust, confirming that dust can dim a beam far more severely than fog. Field studies in semi-arid regions, among them [13], record attenuation spanning roughly 10 to 350 dB/km—a range that lays bare just how punishing dust events are for last-mile optical links.

Three things stand out from this body of work. Most hybrid studies wire up only two of the three tiers and stop short of evaluating the full WDM-PON/FSO/VLC chain end to end. The atmospheric literature on FSO is mature for fog, rain, and turbulence, yet the dust-storm regime peculiar to arid climates is still thinly represented in published end-to-end simulations. And link-budget assessments of three-tier systems with dust attenuation calibrated to real measurements are, for the most part, missing. The present paper takes up all three.

3. System Model

This section sets out the architecture and the governing equations of the proposed three-tier hybrid optical access network. The system is downlink-only and, as Figure 1 shows, is built from three cascaded segments: the WDM-PON fiber backbone (Tier 1), the outdoor FSO link (Tier 2), and the indoor VLC distribution link (Tier 3).

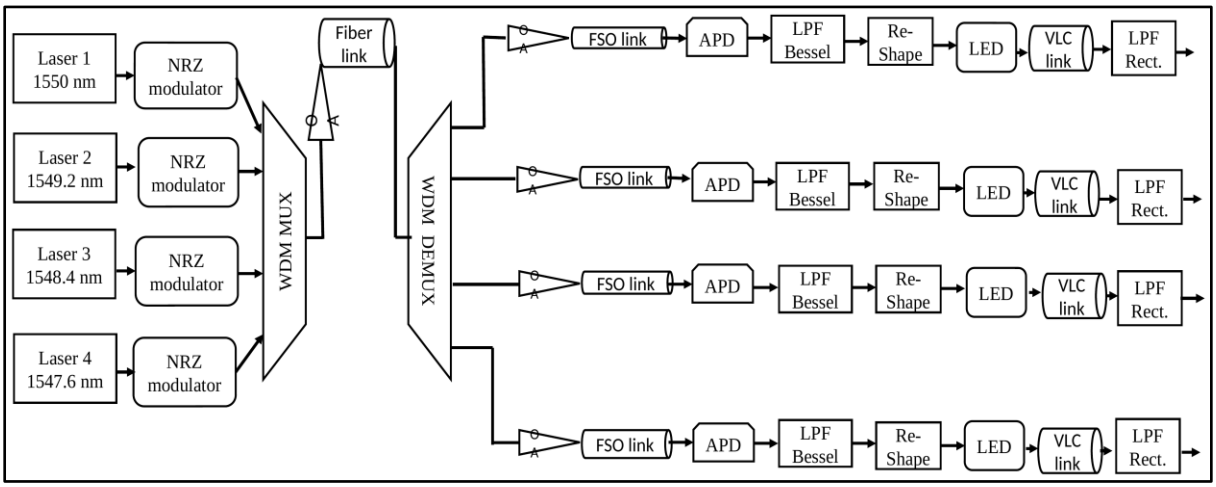

Figure 1. Block diagram of the proposed three-tier hybrid WDM-PON/FSO/VLC optical access network implemented in OptiSystem.

Figure 2 shows the WDM optical spectrum at two points in the chain. In panel (a), taken at the multiplexer output, four well-separated peaks at the assigned wavelengths confirm that the WDM stage is working as intended. Panel (b), captured after 20 km of fiber, shows the same four channels at lower per-channel power, the drop reflecting the cumulative fiber attenuation accrued before amplification.

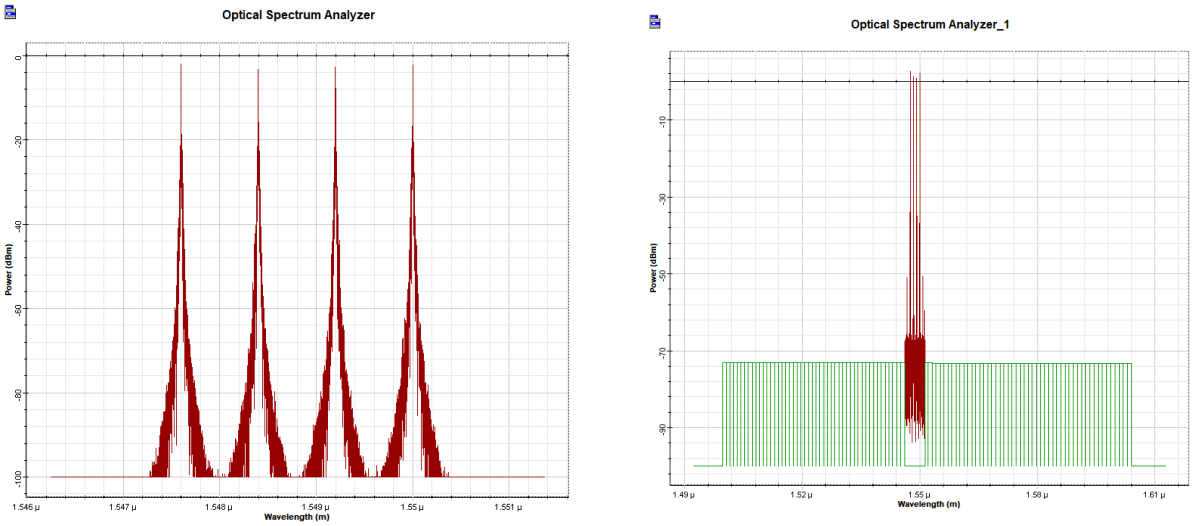

(a) (b)

Figure 2. (a) Optical spectrum at the OLT output (after WDM multiplexer) showing four channels at 100 GHz spacing. (b) Optical spectrum after 20 km of single-mode-fiber propagation.

3.1 Tier 1 — WDM-PON Fiber Backbone

Four continuous-wave lasers sit on the C-band grid at 1550.0, 1549.2, 1548.4, and 1547.6 nm, spaced by 100 GHz in line with the ITU-T G.694.1 recommendation. Each laser drives its own Mach–Zehnder modulator (MZM), which carries an NRZ-OOK pseudo-random bit sequence at 2.5 Gbps per channel. The field at the output of the i-th modulator is written as [19].

$$E_{out,i(t)} = \sqrt{P_i}\sqrt{\frac{1}{2}}\left[1 + \cos\left(\frac{\pi \mathrm{V_{drive(t)}}}{\mathrm{V_\pi}} + \varphi_{bias}\right)\right] e^{j2\pi f_i t} \quad (1)$$

where $\mathrm{P_i}$ is the optical launch power, $\mathrm{V_{drive(t)}}$ is the driving voltage carrying the data stream, $\mathrm{V_\pi}$ is the half-wave voltage of the MZM, φ_{bias} is the bias phase, and $\mathrm{f_i}$ is the optical carrier frequency of the i-th channel.

The four modulated channels are combined by a WDM multiplexer with insertion loss L_{MUX} amplified by EDFA1, and transmitted over a span of single-mode fiber (SMF-28). The received optical power per channel after fiber propagation is [19]

$$P_{rx,fiber} = P_{tx} + G_{EDFA1} - L_{MUX} - \alpha_{fiber} L_{fiber} - L_{DEMUX} \quad (2)$$

Where α_{fiber} is the fiber attenuation coefficient (0.2 dB/km at 1550 nm) and L_{DEMUX} is the demultiplexer insertion loss. The amplified spontaneous emission noise of the EDFA degrades the optical signal-to-noise ratio according to [19]

$$OSNR_{dB} = P_{rx} - NF - 10log_{10}\left(hfB_{ref}\right) - 30 \quad (3)$$

where h is Planck's constant, f is the optical frequency, NF is the amplifier noise figure, and B_{ref} is the reference bandwidth (12.5 GHz for 0.1 nm at 1550 nm).

3.2 Tier 2 — Free-Space Optical Link

Once demultiplexed, each channel passes through a second EDFA and is launched into the outdoor FSO segment, which is represented by the Universal FSO Channel in OptiSystem. The power reaching the FSO receiver is set by the Beer–Lambert law together with the geometric-spreading term [13].

$$P_{rx.FSO} = P_{tx,FSO}\left(\frac{d_R}{d_T+\theta_L}\right)^2 10^{-\alpha_{atm}L/10}\eta_T\eta_R h_{turb} \quad (4)$$

where $P_{tx,FSO}$ is the FSO launch power d_R and d_T are the receiver and transmitter aperture diameters, θ is the beam divergence angle, L is the FSO link length, α_{atm} is the atmospheric attenuation coefficient, η_T and η_R are the optical efficiencies, and h_{turb} is the turbulence-induced channel gain modeled by the Gamma–Gamma distribution [20]

$$f(I) = \frac{2(\alpha\beta)^{(\alpha+\beta)/2}}{\Gamma(\alpha)\Gamma(\beta)}\, I^{\frac{\alpha+\beta}{2}-1}\, K_{\alpha-\beta}\left(2\sqrt{\alpha\beta I}\right) \quad (5)$$

where Γ(·) is the Gamma function, $K_{\alpha-\beta}(.)$ is the modified Bessel function of the second kind, and α and β are the large- and small-scale turbulence parameters determined by the refractive-index structure parameter ${C^2}_n$ and the Rytov variance [20]

$${\sigma^2}_R = 1.23{C^2}_n\, k^{7/6}L^{11/6} \quad (6)$$

with k = 2π/λ the optical wave number. At the FSO receiver, an avalanche photodiode (APD) converts the optical signal to electrical current, followed by a fourth-order Bessel low-pass filter. The total electrical noise comprises shot, thermal, and beat-noise contributions [18]

$${\sigma^2}_{total} = 2qIM^2F(M)B + \frac{4k_BT}{R_L}B + {\sigma^2}_{ASE} \quad (7)$$

where q is the electron charge, I is the photocurrent, M is the APD multiplication factor, F(M) is the excess noise factor, k_B is Boltzmann's constant, T is the absolute temperature, $R_L$is the load resistance, and ${\sigma^2}_{ASE}$ is the amplifier beat-noise variance.

3.3 Tier 3 — Visible Light Communication Link

A 3R regenerator is placed between the FSO receiver and the VLC transmitter to reamplify, reshape, and retime the signal; it stands in for the optoelectronic regeneration that occurs at the optical network unit (ONU), where the arriving signal is detected and a clean optical signal is relaunched into the indoor VLC channel. This regenerated signal drives a 550 nm LED, and the power collected at the VLC photodetector is [21].

$$P_{rx,VLC} = P_{LED}G_{OWC}\,\eta_{T,VLC}\,\eta_{R,VLC}\,10^{-L_{add,vlc}/10} \quad (8)$$

where P_{LED} is the LED optical power, G_{OWC} is the geometric channel gain, $\eta_{T,VLC}$ and $\eta_{R,VLC}$ are the VLC optical efficiencies, and $L_{add,vlc}$ accounts for additional indoor losses. The recovered signal at the PIN photodetector is filtered and analyzed by a BER analyzer that computes the end-to-end bit error rate, quality factor, and eye-diagram statistics.

3.4 End-to-End Power-Budget Model

To track how optical power evolves from the OLT launch all the way to the VLC receiver, we assemble a complete end-to-end power budget. Expressed in decibels, the power at the VLC photodetector is the launch power plus the amplifier gains, less the component, fiber, and geometric losses accumulated across the three tiers.

$$P_{rx}^{dBm} = P_{tx} + \sum_{m=1}^{2} G_{EDFA,m} - \sum_i L_{comp,i} - \sum_j \alpha_j L_j - L_{geo}^{FSO} - L_{geo}^{OWC} \quad (9)$$

where P_{tx} is the OLT launch power, $G_{EDFA,m}$ are the gains of the two EDFAs, $L_{comp,i}$ are the lumped component insertion losses (MUX, DEMUX, and additional losses), $\alpha_j\ L_j$ are the fiber and atmospheric attenuation terms, and L_{geo}^{FSO} and L_{geo}^{OWC} are the geometric (beam-spreading and free-space-path) losses of the FSO and OWC channels, respectively.

4. Simulation Setup

The system was implemented and simulated in OptiSystem with the parameters collected in Table 1. A reference wavelength of 1550 nm, the same parameters are held across all five atmospheric scenarios; the only quantities that change from one scenario to the next are the FSO channel attenuation and the refractive-index structure parameter ($C^2{}_n$). The parameter sweeps over FSO distance, bit rate, fiber length, and VLC range are all run at the clear-weather baseline.

Table 1. Simulation parameters of the proposed three-tier hybrid system.

Parameter	Value
Number of WDM channels	4
Channel spacing	100 GHz (0.8 nm)
Channel wavelengths	1547.6, 1548.4, 1549.2, 1550.0 nm
CW laser launch power	10 dBm
Modulation format	NRZ-OOK (Mach–Zehnder)
Bit rate per channel	2.5 Gbps
EDFA1 / EDFA2 gain	10 dB / 10 dB
EDFA noise figure	4 dB
Fiber type / length	SMF-28 / 20 km
Fiber attenuation / dispersion	0.2 dB/km / 16.75 ps·nm^{-1}·km^{-1}
Fiber Nonlinearity	ON
MUX / DEMUX insertion loss	1.5 dB / 1.5 dB
FSO baseline distance	1 km
FSO Tx/Rx aperture	5 cm / 10 cm
FSO beam divergence	2 mrad
FSO Tx/Rx efficiency	0.8 / 0.8
FSO turbulence model	Gamma–Gamma
VLC LED wavelength	550 nm

VLC link distance	3 m
VLC Tx/Rx aperture	1 cm / 1 cm
VLC Tx / Rx efficiency	0.7 / 0.7

5. Results and Discussion

5.1 Baseline Performance Under Clear Weather

We begin with the baseline under clear weather (atmospheric attenuation 0.43 dB/km, $C^2{}_n$ = 5 × 10^{-15}). Figure 3 collects the end-to-end eye diagrams of the four WDM channels at the VLC output; the clean, wide-open apertures confirm error-free transmission right across the WDM grid. The measured metrics are: Channel 1, BER = 1.86 × 10^{-13}, Q = 7.25; Channel 2, BER = 4.46 × 10^{-12}, Q = 6.80; Channel 3, BER = 4.17 × 10^{-11}, Q = 6.47; and Channel 4, BER = 4 × 10^{-16}, Q = 8.00. Every channel lies comfortably below the 10^{-9} error-free threshold.

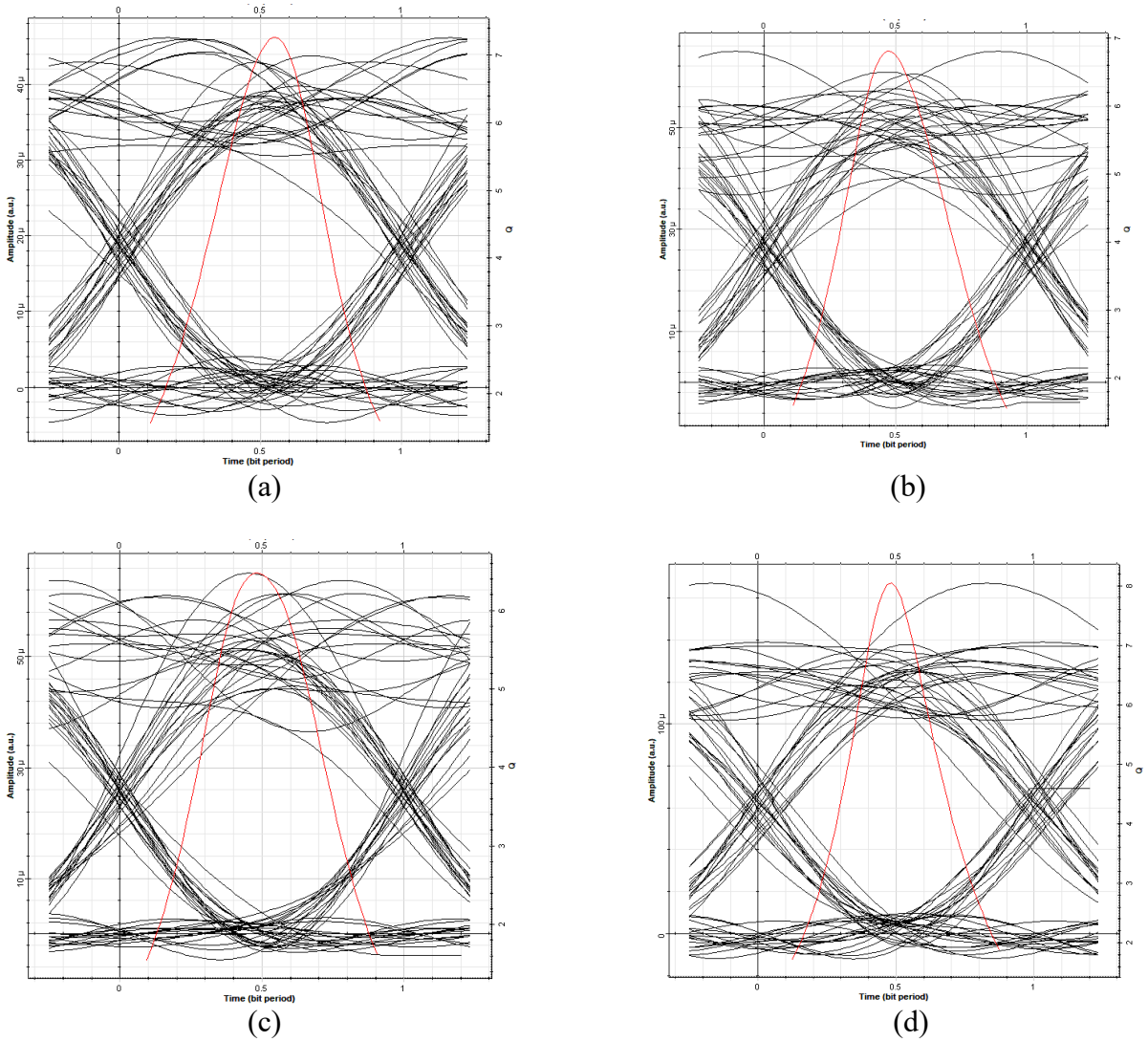

Figure 3(a) Eye diagram of Channel 1 (1550 nm) under clear weather. (b) Eye diagram of Channel 2 (1549.2 nm) under clear weather. (c) Eye diagram of Channel 3 (1548.4 nm) under clear weather. (d). Eye diagram of Channel 4 (1547.6 nm) under clear weather.

Although the end-to-end BER ranges over several orders of magnitude across the four channels (from 4×10^{-16} to 4.17×10^{-11}), all of them stay far under the 10^{-9} error-free threshold, which confirms sound baseline operation. The small channel-to-channel spread reflects the wavelength dependence of the EDFA gain spectrum and of the MUX/DEMUX response rather than any systematic ordering across channels.

5.2 Performance Under Degraded Atmospheric Conditions

Adding light haze (4.2 dB/km) is enough to drop the Q factors beneath the error-free threshold, though the channels stay under the FEC limit of 3.8×10^{-3}. The four channels then read 1.15×10^{-7}, 2.28×10^{-6}, 1.00×10^{-5}, and 1.2×10^{-6}, all still within reach of FEC. Once dust haze (10 dB/km) sets in, the received power drops below the APD sensitivity, and every channel fails; the light dust storm (29 dB/km) and the heavy dust storm (127 dB/km) end the same way.

In the worst case—the heavy dust storm—the eye diagrams collapse, as Figure 4 shows. The apertures have closed completely—the opposite of the open eyes in Figure 3—a clear visual signature of total signal loss. Read side by side, Figures 3 and 4 bracket the dynamic range of the system between its best and worst operating points.

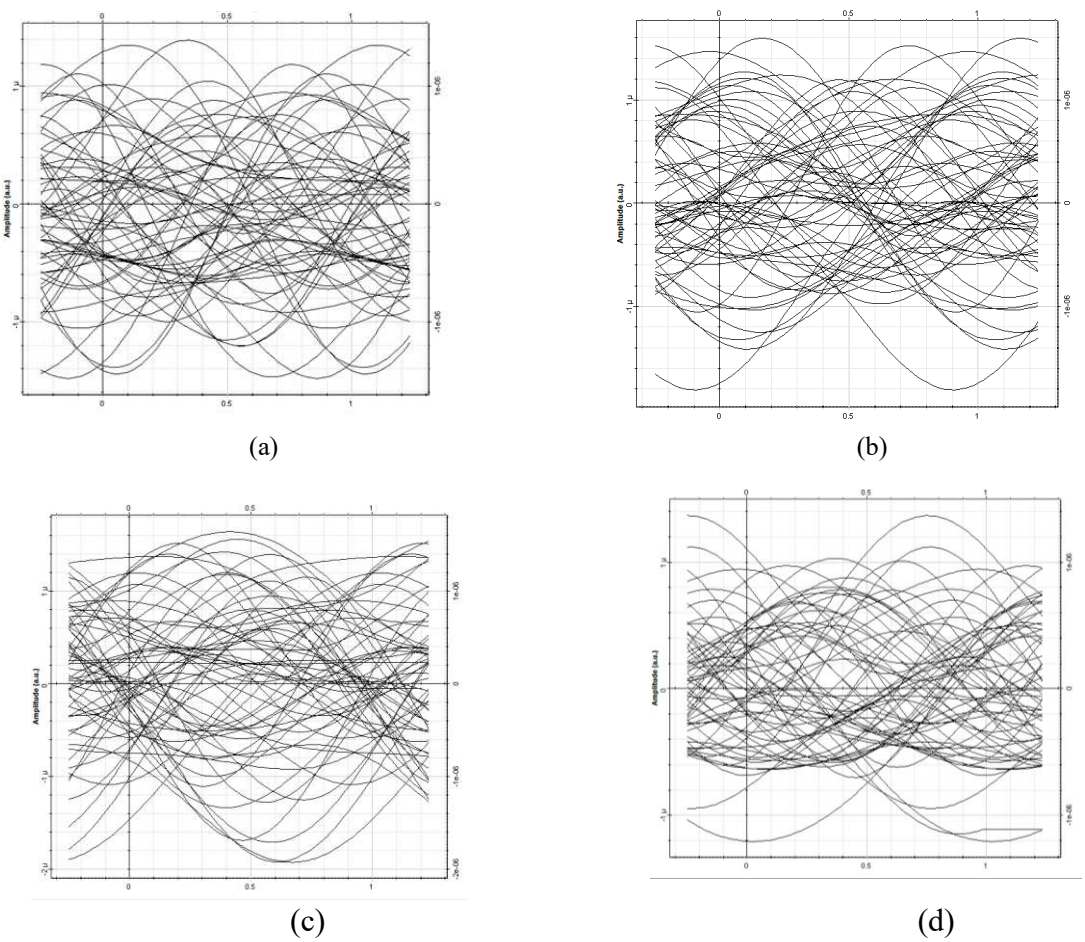

Figure 4 (a) Eye diagram of Channel 1 under heavy dust storm (127 dB/km). (b) Eye diagram of Channel 2 under heavy dust storm. (c) Eye diagram of Channel 3 under heavy dust storm. (d) Eye diagram of Channel 4 under heavy dust storm.

Plotted on a logarithmic scale against atmospheric condition, with the error-free and FEC thresholds marked for reference, the BER of all four channels follows an abrupt trend (Figure 5): error-free under clear weather, FEC-recoverable under light haze, and outright failure once attenuation passes roughly 10 dB/km over the 1 km FSO span. The four curves stay close together, a sign that performance is set by the aggregate atmospheric attenuation rather than by any per-channel wavelength dependence.

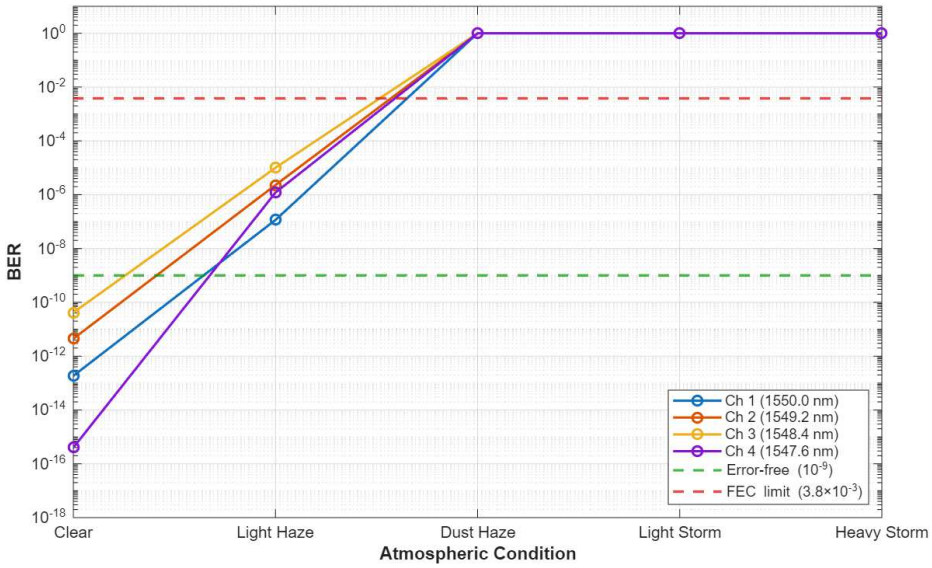

Figure 5. BER versus atmospheric condition for the four WDM channels over the 1 km FSO + 20 km fiber link.

The companion Q-factor data tell the same story (Figure 6). Under clear skies every channel clears the Q = 6 mark. Light haze pulls the Q factor down to 4.3–5.2—below the error-free line, but still inside the FEC-recoverable band—while the three severe cases drive it to zero, matching the link failures already seen in Figure 5.

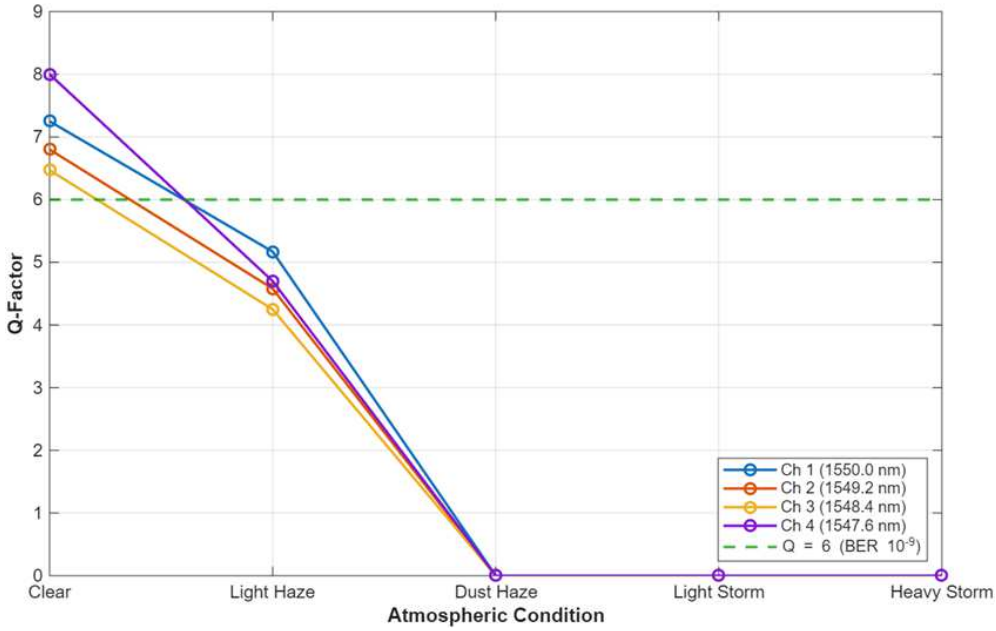

Figure 6. Q-factor versus atmospheric condition for the four WDM channels. The reference at Q = 6 corresponds to BER = 10^{-9}.

5.3 Effect of FSO Link Distance

Under clear weather, BER holds up across most of the FSO span (Figure 7). From 100 m to 1000 m every channel stays deep in the error-free regime, the BER climbing only gently. Past 1000 m the picture changes fast: at 1200 m the channels slip over the error-free threshold but remain under the FEC limit, and by 1300 m they sit at or above it. From 1500 m onward every channel fails. The usable clear-sky FSO reach, then, is about 1200–1300 m.

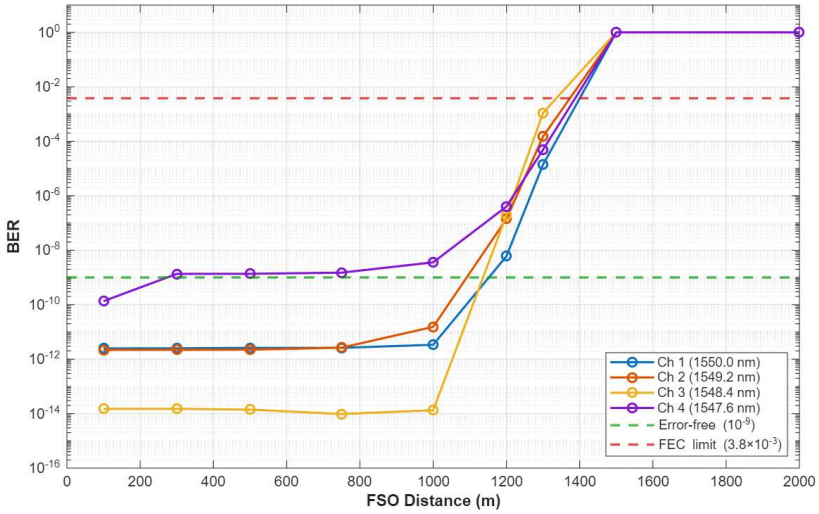

Figure 7. BER versus FSO link distance for the four WDM channels under clear weather (fiber = 20 km).

Figure 8 is the study's central result: the BER of Channel 1 traced against FSO distance for all five weather conditions. As attenuation grows, the error-free reach falls steadily—about 1000 m under clear weather, 750 m under light haze, 500 m under dust haze, 200 m under a light storm, and under 200 m in a heavy storm. This curve captures the trade-off between range and atmospheric severity, and it is the design guideline we lean on for last-mile FSO in arid settings.

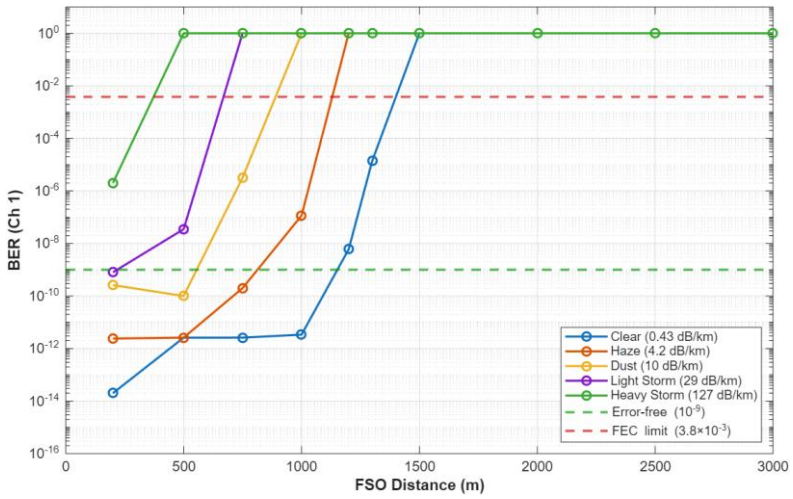

Figure 8. BER of Channel 1 versus FSO link distance under five weather conditions (key design-guideline figure).

Distilled to a single chart, the maximum usable FSO distance for each weather condition at two reliability thresholds falls steadily with attenuation (Figure 9)—a compact design reference. At the typical 1 km terminal spacing, holding the link through a dust event therefore calls for either an adaptive cut in distance or a complementary RF backup—a conclusion that lines up with the measured dust-attenuation figures reported for arid environments [13], [15].

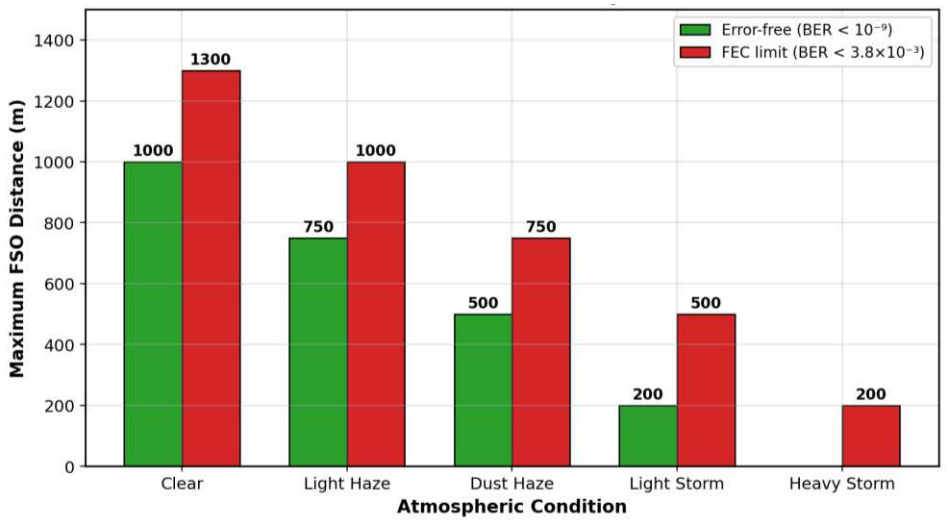

Figure 9. Maximum achievable FSO link distance under each weather condition at the error-free and FEC thresholds.

5.4 Effect of Transmission Bit Rate

Sweeping the line rate over 0.625, 1.25, 2.5, 5, and 10 Gbps at baseline gives the trends in Figure 10. BER worsens monotonically as the symbol rate climbs, as one would expect. Up to 2.5 Gbps, every channel holds a BER of order 10^{-11} or better. At 5 Gbps, Channels 1–3 edge past the error-free threshold but stay under the FEC limit, while Channel 4 remains error-free. By 10 Gbps all channels are at or beyond the FEC limit, marking the practical ceiling for reliable operation. The system thus carries a solid per-channel rate of about 5 Gbps—an aggregate near 20 Gbps over the four channels—before FEC becomes indispensable.

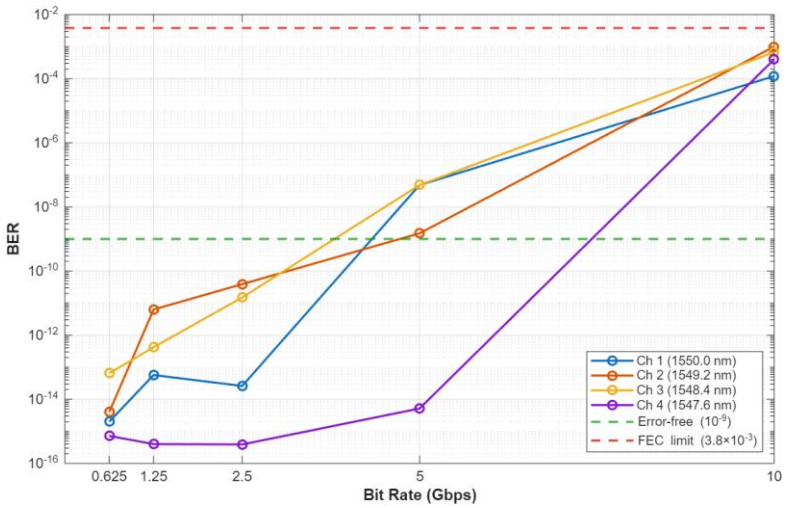

Figure 10. BER versus transmission bit rate for the four WDM channels under baseline conditions.

5.5 Effect of Fiber Length

Sweeping the SMF length from 5 km to 30 km at baseline traces how BER tracks fiber reach (Figure 11). The channels keep BER below 10^{-11} out to 20 km, beyond which a moderate rise sets in. The largest change is in Channel 4 at 30 km (BER $\approx 3 \times 10^{-8}$), where the combined weight of fiber attenuation and chromatic dispersion is felt most. The 20 km baseline matches the reach typically specified for GPON/XG-PON.

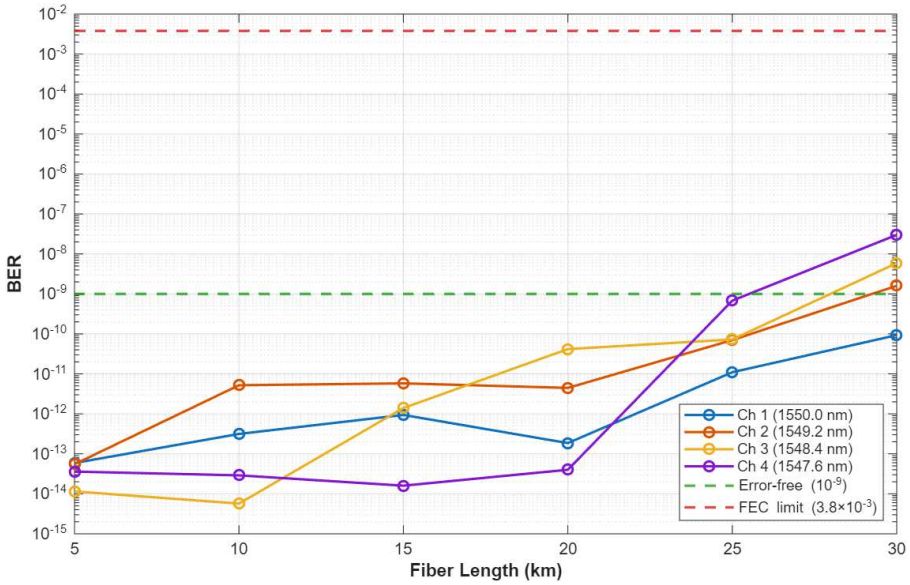

Figure 11. BER versus SMF fiber length for the four WDM channels under baseline conditions.

5.6 Effect of VLC Indoor Distance

Across the 1 m to 5 m indoor span, the BER behaves as in Figure 12. Channels 1–3 stay error-free over the whole range, while Channel 4 is more sensitive, its BER rising from 1.5×10^{-9} at 1 m to 3.8×10^{-8} at 5 m. That gentle slope is the mark of a benign indoor channel: here the budget is set by geometric coupling loss, not atmospheric impairment, which is exactly why the VLC tier suits indoor last-meter distribution.

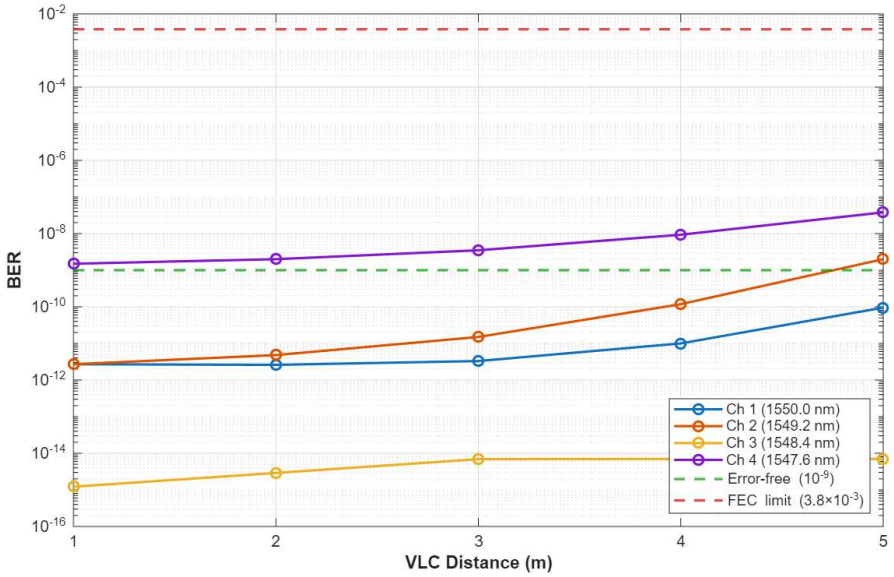

Figure 12. BER versus VLC indoor link distance for the four WDM channels under baseline conditions.

6. Link Budget Analysis

Substituting the baseline parameters of Table 1 into the power-budget model of Equation (9) gives the term-by-term optical budget set out in Table 2.

Table 2. End-to-end optical power budget of the three-tier system under baseline conditions.

Component	Gain/Loss (dB)	Cumulative Power (dBm)
CW Laser (OLT launch)	+10	+10.00
WDM MUX	−1.5	+8.50
EDFA1	+10	+18.50
SMF-28 (20 km × 0.2 dB/km)	−4.0	+14.50
WDM DEMUX	−1.5	+13.00
EDFA2	+10	+23.00
FSO atmospheric + additional	−2.43	+20.57
FSO geometric + FSPL	−20.1	+0.47
OWC geometric + FSPL	−10.0	−9.53
OWC additional loss	−3.0	−12.53
Final power at VLC PIN	—	−12.53

7. Optical Received Power

Figure 13 shows the simulated received optical power at the main interfaces of the system, and the agreement with the analytical budget of Table 2 is close. What small discrepancies remain trace back to the wavelength-dependent gain ripple of the EDFAs and to the full simulation of the Gamma–Gamma turbulence channel.

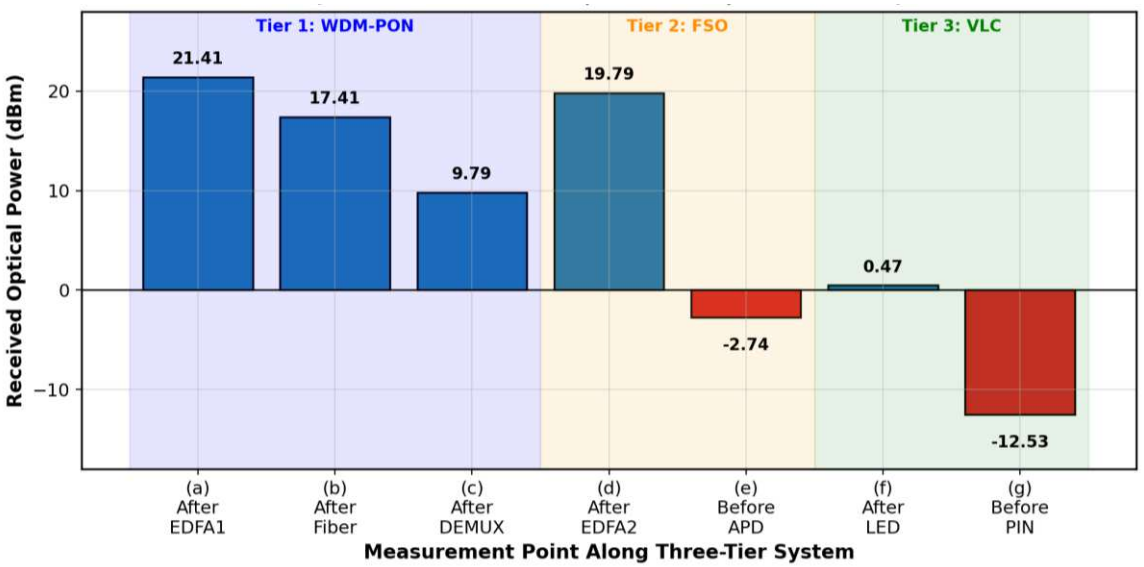

Figure 13. Simulated received optical power at the principal interfaces of the three-tier system, consistent with the analytical link budget.

8. Conclusion

This paper has analyzed, end to end, a hybrid three-tier WDM-PON/FSO/VLC access network intended for last-mile connectivity in arid climates. The architecture brings together a four-channel, 100 GHz-spaced WDM-PON backbone over 20 km of single-mode fiber, an outdoor 1 km FSO segment modeled with Gamma–Gamma turbulence, and a 3 m indoor visible-light link, the whole of it built and simulated in OptiSystem.

Several findings stand out. Under the clear-weather baseline, all four WDM channels run error-free (BER below 10^{-9}) with Q factors between 6.47 and 8.00. Once the atmosphere degrades, the FSO segment is plainly the tier that governs performance: light haze drops the system to FEC-recoverable operation, and dust events at 10 dB/km or more break the link entirely at the 1 km FSO distance. The usable FSO reach shrinks from roughly 1000 m under clear weather to under 200 m in a heavy dust storm. On the capacity side, the system carries a per-channel rate near 5 Gbps (about 20 Gbps in aggregate) before FEC is required, and it absorbs fiber lengths up to 20 km and indoor VLC ranges up to 5 m with little penalty. The cumulative link budget lands at −12.53 dBm at the VLC photodetector, in line with the simulated values.

Together these results give a quantitative footing for designing last-mile optical access in dust-prone arid environments, and they make clear that the FSO tier is where the engineering effort belongs. We see several lines for future work: validating the simulated attenuation values against field measurements taken during actual dust storms; adding adaptive power control and adaptive modulation; introducing a bidirectional uplink; and using machine learning to forecast channel impairment so that traffic can be routed in real time between the FSO link and a complementary RF backup.

***Funding:** This research received no external funding.

***Corresponding author**:
Adnan Ali Abdullah
Shirqat College of Engineering, Department of Electrical Engineering, University of Tikrit, Shirqat, Iraq
Email: adnan.ali23@tu.edu.iq

References

[1] S. M. El-Garhy, A. A. M. Khalaf, M. Abaza, and M. H. Aly, "Intelligent transportation system using wireless optical communication: a comparative study," Optical and Quantum Electronics, vol. 56, no. 2, p. 247, 2024.

[2] A. Lamba, J. Sehgal, M. Kumar, and E. Akanksha, "A fiber-wireless integration approach in WDM-PON architecture, boosted with polarization multiplexing and optical frequency comb source," Journal of Optical Communications, vol. 46, no. 3, pp. 565–574, 2025.

[3] M. Kumari, "Investigation of 16 × 10 Gbps mode division multiplexed enabled integrated NGPON–FSO architecture under wired-wireless link losses," Journal of Optical Communications, vol. 46, no. 2, pp. 347–355, 2025.

[4] A. K. Singh and R. Pandey, "Exploring visible light communication for real-time indoor metaverse connectivity," Journal of Optical Communications, vol. 47, no. 2, pp. 435-446, 2025.

[5] K. Kaur and H. Singh, "Free space optical communication system under different weather conditions," Journal of Optical Communications, vol. 44, no. 1, pp. 103-110, 2023.

[6] D. AlQahtani and F. El-Nahal, "Coherent WDM-PON and free space optical (FSO) system for front-haul in next-generation cellular networks," Optik, vol. 323, p. 172212, 2025.

[7] D. AlQahtani and F. El-Nahal, "WDM-PON free space optical (FSO) system utilizing LDPC decoding for enhanced cellular C-RAN fronthaul networks," Photonics, vol. 12, no. 4, p. 391, 2025.

[8] Wu T-H, Liao C-Y, Yeh C-H, Chen Y-W, Kao Y-H, Lin S-Y, Lin Y-H, Liaw S-K, "A self-healing WDM access network with protected fiber and FSO link paths effective against fiber breaks," Photonics, vol. 12, no. 4, p. 323, 2025.

[9] M. Kumari, V. Arya, and H. M. R. Al-Khafaji, "8 × 200 Gbps hybrid PON and digital filter multiple access incorporating fiber-FSO link impairments in a wheel architecture," International Journal of Communication Systems, 2025.

[10] M. Kumari and V. Arya, "Four Laguerre–Gaussian mode-division multiplexed incorporated hybrid XG-PON and FSO Gamma-Gamma fading system under severe weather conditions," Optical and Quantum Electronics, vol. 56, no. 1, p. 113, 2024.

[11] M. A. Esmail, "Unified performance analysis of free-space optical systems over dust-induced fading channels," Electronics, vol. 14, no. 23, p. 4637, 2025.

[12] M. Mrabet, and M. Sliti, "Performance analysis of FSO communications in desert environments," Optical and Quantum Electronics, vol. 56, p. 315, 2024.

[13] B. M. Rasool, S. O. Hasan, and R. Z. Yousif, "Enhanced free space optical communication in semi-arid climates based on adaptive M-signals level PAM modulation utilizing EAM modulator for last-mile connectivity in Kurdistan-Iraq region: Erbil and Sulaimani case studies," Journal of Optics, (2026). https://doi.org/10.1007/s12596-026-03113-2

[14] M. A. A. Ali, Z. H. Baqi, and S. Kh. Rahi, "Investigation and analysis of data rate for free space optical communications system under dust conditions," Wireless Personal Communications, vol. 113, no. 4, pp. 2327–2338, 2020.

[15] M. A. Esmail, A. M. Ragheb, H. A. Fathallah, M. Altamimi, and S. A. Alshebeili, "5G-28 GHz signal transmission over hybrid all-optical FSO/RF link in dusty weather conditions," IEEE Access, vol. 7, pp. 24404–24410, 2019.

[16] F. M. Elamrawy, A. Abd El Aziz, S. Khamis, and H. Kasem, "Performance analysis of an indoor visible light communication system using LED configurations and diverse photodetectors," Scientific Reports, vol. 15, no. 1, p. 16064, 2025.

[17] V. V. Belgaonkar, C. L. Triveni, and R. Sundaraguru, "Free space optical communication using OQPSK in the presence of strong atmospheric turbulence and losses," Optical and Quantum Electronics, vol. 56, no. 10, p. 1669, 2024.

[18] Z. Xu, G. Xu, and Z. Zheng, "BER and channel capacity performance of an FSO communication system over atmospheric turbulence with different types of noise," Sensors, vol. 21, no. 10, p. 3454, 2021.

[19] G. P. Agrawal, Fiber-Optic Communication Systems, 4th ed. Hoboken, NJ: Wiley, 2010.

[20] L. C. Andrews and R. L. Phillips, Laser Beam Propagation Through Random Media, 2nd ed. Bellingham, WA: SPIE Press, 2005.

[21] A. Poulose, "Simulation of an indoor visible light communication system using OptiSystem," Signals, vol. 3, no. 4, pp. 765–793, 2022.